INSTITUTE OF PHYSICS PUBLISHING JOURNAL OF PHYSICS B: ATOMIC, MOLECULAR AND OPTICAL PHYSICS

J. Phys. B: At. Mol. Opt. Phys. **39** (2006) 5105–5117 doi:10.1088/0953-4075/39/24/008

Absolute cross sections for electron impact ionization and dissociation of O_2^+

H Cherkani-Hassani[1], D S Belic[1,3], J J Jureta[1,2] and P Defrance[1]

[1] Department of Physics, Catholic University of Louvain, Chemin du Cyclotron 2, B-1348 Louvain-la-Neuve, Belgium
[2] Institute of Physics, PO Box 68, 11081 Belgrade, Serbia
[3] Faculty of Physics, PO Box 386, 11000 Belgrade, Serbia

Received 18 July 2006, in final form 18 October 2006
Published 23 November 2006
Online at stacks.iop.org/JPhysB/39/5105

Abstract

Absolute cross sections for electron impact single ionization, dissociative excitation and dissociative ionization of O_2^+ were measured in the energy range from threshold to about 2.5 keV by means of a crossed beam set-up. The analysis of product velocity distributions has been applied in order to (i) separate the three processes and (ii) determine the kinetic energy release distribution of ionic fragments. Dissociation is seen to dominantly follow the ionization and the excitation processes, the maximum of the cross sections being found to be $(2.20 \pm 0.09) \times 10^{-17}$ cm^2, $(5.3 \pm 1.0) \times 10^{-17}$ cm^2 and $(22.0 \pm 4.6) \times 10^{-17}$ cm^2 for simple ionization, dissociative ionization and dissociative excitation, respectively. The total kinetic energy released to the fragments is seen to extend up to about 20 eV.

1. Introduction

As oxygen is a major constituent of the Earth's atmosphere, and of stellar and laboratory plasmas, there is still a large scientific interest to investigate the processes involving both its atomic and molecular species and their ions. In spite of this situation, little has been published about electron interaction with the oxygen molecular ion, which plays an important role in chemical and atmospheric reactions through interactions with other atomic particles, electrons and photons.

First, cross section measurements of O^+ formation by electron impact on O_2^+ were performed by Van Zyl and Dunn (1967) and, more recently, Peverall *et al* (2001) have measured cross sections for electron impact dissociative recombination (DR) and dissociative excitation (DE) of O_2^+, by detection of neutral oxygen atoms.

The paucity of these investigations is related to a number of experimental difficulties. For instance, it is hard to produce ions in given electronic and vibrational levels. Next, after

the collision, molecular ions usually dissociate in a wide energy and angular range and it is difficult to collect all of them at once. In addition, in the case of homonuclear diatomic molecules, fragment ions are produced with the same charge-to-mass ratio, so that they cannot be identified by means of standard electrostatic or magnetic devices.

In this paper we report on results of absolute cross section measurements for electron impact ionization and dissociation of the O_2^+ ion in the energy range from threshold to 2.5 keV. The following reactions are considered:

$$O_2^+ + e^- \rightarrow O_2^{2+} + 2\,e^- \tag{1}$$

$$\rightarrow O^+ + O + e^- \tag{2}$$

$$\rightarrow O^+ + O^+ + 2\,e^-. \tag{3}$$

Reactions (1), (2) and (3) represent single ionization (SI), dissociative excitation (DE) and dissociative ionization (DI), respectively, and the corresponding cross sections are σ_{SI}, σ_{DE} and σ_{DI}. The analysis of product velocity distributions is applied in order to (i) separate the three processes and (ii) determine the kinetic energy release distribution (KERD) of fragment ions, which reflect the role of intermediate states formed in reactions (1)–(3): no KER for (1), a low one for (2) and a bigger one for (3).

2. Experimental method and apparatus

In this experiment the animated crossed electron–ion beam method is applied (Defrance *et al* 1981). Both the present apparatus and the experimental method have been recently described in detail (Lecointre *et al* 2006) and only a brief outline is presented here.

2.1. Experimental set-up

In the apparatus, the fixed energy molecular ion beam interacts at right angles, with an electron beam whose energy may be tuned from a few eV up to 2.5 keV. Ions are extracted from a Penning (PIG) ion source and accelerated to 8 keV. The ion beam is selected by means of a double focusing 90° magnetic analyser, additionally focused and purified by a 45° spherical electrostatic deflector and directed into the collision region where it crosses the ribbon-shaped electron beam, at right angles. Product ions are separated from the primary ion beam by means of a double focusing 90° magnetic analyser. Due to the transfer of internal potential energy, dissociation fragments exhibit both broad velocity and angular distributions in the laboratory frame. At the fixed ion velocity, selected by the variable analyser slit, the angular acceptance of the magnet (0.1 radian) is large enough to convey all the ions to the detector, with the maximum expected KER produced by dissociation processes. Product ions are further deflected by a 90° electrostatic spherical deflector and directed onto a channeltron detector.

2.2. Cross section measurements

In the animated beam method (Defrance *et al* 1981), the electron beam is swept across the ion beam in a linear seesaw motion at a constant speed u. The total number of events K produced during one complete electron beam movement is related to the cross section (σ) by the following expression:

$$\sigma = \frac{uK}{AI_eI_i\gamma} \tag{4}$$

where γ is the detector efficiency, I_e and I_i are the electron and ion beam current intensities, respectively, and A is a kinematic factor, which is given for beams interacting at right angles:

$$A = \frac{\left(v_e^2 + v_i^2\right)^{1/2}}{v_e v_i q_i e^2}. \tag{5}$$

In this expression, e and $q_i e$ and v_e and v_i are the charges and velocities of electrons and ions, respectively. Assuming $m_i \gg m_e$, the true interaction energy E_e (eV) is given by

$$E_e = V_e + \frac{m_e}{m_i}(q_i V_i - V_e) \tag{6}$$

where V_e and V_i, and m_e and m_i are the acceleration voltages and masses of electrons and ions, respectively. The electron energy is corrected for a contact potential difference.

2.3. Total cross sections and kinetic energy release distributions

The angular acceptance of the magnet analyser allows the total transmission of the angular distribution of product fragments emitted at a given velocity v, in the laboratory frame. This velocity is defined by the magnetic field $B(v = qRB/m)$ and it is also given by $\sqrt{v_c^2 + w^2 + 2v_c w\cos\theta_L}$, where v_c, θ_L and w represent the centre of mass velocity, the ejection angle in the laboratory and the fragment velocity in the centre-of-mass frame, respectively. Here, m and q are the fragment ion mass and charge respectively, and R is the radius of its trajectory in the analyser magnetic field.

Due to the KER, the velocity distribution ($f(v) = \mathrm{d}\sigma(v)/\mathrm{d}v$) usually exceeds the corresponding magnetic analyser acceptance, which is essentially defined by the size of the analysing slits. As a consequence, total transmission of dissociation products to the detector cannot be achieved. In order to put the cross section on the absolute scale, the velocity distribution must be determined and integrated over the full velocity range. For this purpose, first, the apparent cross section $\sigma_m(B)$ is measured at a given electron energy, as a function of the analyser magnetic field (B). Next, the corresponding differential cross section, $(\mathrm{d}\sigma(B)/\mathrm{d}B)$, is computed (Lecointre *et al* 2006) and the velocity distribution is given by

$$f(v) = \frac{\mathrm{d}\sigma(v)}{\mathrm{d}v} = \frac{m}{qR}\frac{\mathrm{d}\sigma(B)}{\mathrm{d}B}. \tag{7}$$

The total cross section is computed by integrating the distribution over the full velocity range:

$$\sigma = \int_0^\infty f(v)\,\mathrm{d}v. \tag{8}$$

It was demonstrated (Lecointre *et al* 2006) that the KERD may be expressed in terms of the velocity distribution by

$$\frac{\mathrm{d}\sigma(E_{KER})}{\mathrm{d}E_{KER}} = \frac{-2\mu v_c}{m^2(1-\varepsilon/2)}\frac{\mathrm{d}}{\mathrm{d}v}\left(\frac{1}{v}\frac{\mathrm{d}\sigma(v)}{\mathrm{d}v}\right) \tag{9}$$

where μ is the reduced mass of the fragment. In the present experiment, ε is expressed as

$$\varepsilon = 2\left(1 - \frac{2v_c}{\sigma}\int_{v_c}^\infty \frac{1}{v}\frac{\mathrm{d}\sigma(v)}{\mathrm{d}v}\,\mathrm{d}v\right). \tag{10}$$

This quantity is seen to characterize the angular distribution of dissociation products with respect to the velocity of the incident electron, due to the initial orientation of the molecular axis.

The total kinetic energy released (E_{KER}) to dissociation fragments is given by

$$E_{KER} = \frac{m^2 w^2}{2\mu}. \tag{11}$$

2.4. Experimental procedure

As described above, at a fixed v, only a fraction (η) of the fragment velocity distribution is detected at once. To overcome this problem, the above-mentioned magnetic field scans are performed at fixed electron energies. The repetition of this procedure at each electron energy results in a very long and tedious task. In order to reduce it with little effect on the accuracy of final results, an alternative procedure (Bahati *et al* 2001) was introduced to cover the whole energy range without measuring all the distributions. In the first step, the apparent cross section $\sigma_{\mathrm{m}}(B_0)$ is measured versus the electron energy at the magnetic field B_0 which corresponds to the centre of the velocity distribution, that is to the detection of fragments with $v = v_{\mathrm{c}}$. Working at this field is necessary in order to include the contributions of all the ejection speeds in the centre-of-mass frame. The absolute cross section is related to the apparent one by

$$\sigma = \sigma_{\mathrm{m}}(B_0)/\eta. \tag{12}$$

To put the apparent cross section $\sigma_{\mathrm{m}}(B_0)$ on the absolute scale over the whole electron energy range, the transmission factor is first computed at the selected electron energies where magnetic field scans are performed. Next, these results are interpolated and extrapolated in order to estimate η at any electron energy and the apparent cross section is corrected by means of (12) to obtain the absolute cross section.

2.5. Separation of SI, DE and DI

Products of reactions (1)–(3) form a single distribution whose shape depends on the electron energy, i.e. on the various involved KERs. In the present experiment, magnetic field scans were recorded at 8 incident electron energies (4.5, 10.5, 13.5, 18.5, 38.5, 78.5, 148.5 and 498.5 eV).

At low energies, below the ionization threshold (figure 1(a)), only DE is observed. The width of the spectra is seen to increase significantly (up to 5 mT) with the electron energy, as a consequence of the larger kinetic energy released to the fragments, associated with the opening of new possible reaction channels.

Above the ionization threshold (figure 1(b)), a narrow feature (FWHM: 0.8 mT) located in the middle of the spectrum is superimposed on a broad distribution. The product ions forming this narrow peak are species with unaffected ($v = v_{\mathrm{c}}$), quasi-monokinetic ($w = 0$), velocity distribution. This contribution obviously originates from SI (process 1). The broad part of the spectrum (up to 10 mT), corresponding to large ejection speeds, evidently finds its origin in both the DE and the DI dissociation processes (processes 2 and 3, respectively). The broadening of the spectra is due to Coulomb repulsion experienced by DI fragments. A close examination of the spectra confirms this statement and their analysis allows the determination of the transmission factors, which are needed to determine the cross sections for SI, DE and DI, separately.

Cross sections versus electron energy are measured for three different values of the analyser magnetic field: at 108.5 mT (B_0, σ_{m0}), where the three contributions are present, at 109 mT (σ_{m1}), where DE and DI contribute and at 114 mT (σ_{m2}) where only DI is expected.

The procedure to separate the individual contributions of the three identified processes was developed previously for the N_2^+ molecular ion (Bahati *et al* 2001). This is illustrated in the present case for 148.5 eV (figure 1(c)). First, σ_{SI} is determined as the difference between σ_{m0} and σ_{m1}. Next, the pure DI signal is isolated by fitting the outer part of the spectrum (from 102 to 104 mT and from 113 to 115 mT). The fitting curve (curve 1 in figure 1(c)) allows the determination of the DI transmission factor (η_{DI}), which is seen to be close to 10% in the

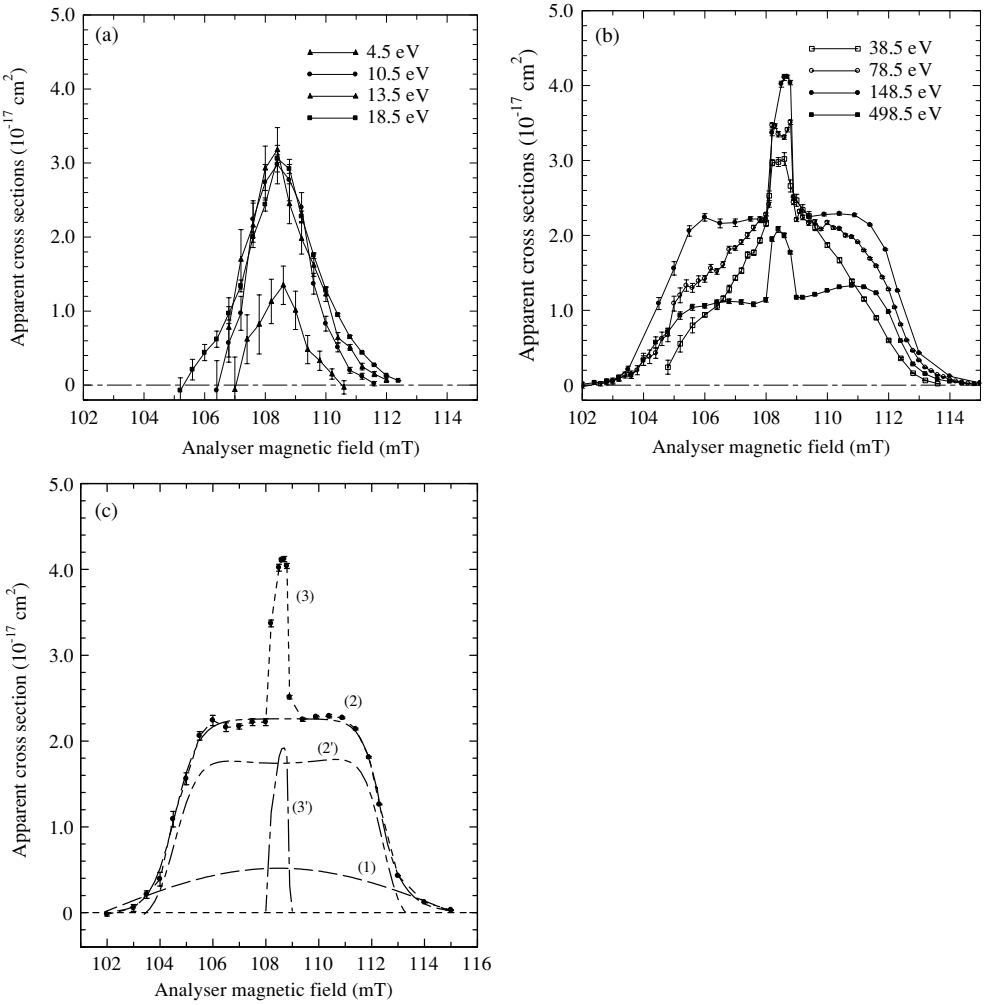

Figure 1. (a) Magnetic field scans of the apparent cross section at selected electron energies, below the SI threshold. (b) Magnetic field scans of the apparent cross section at selected electron energies, above the SI threshold. (c) Data of (b) ($E_e = 148.5$ eV) and fitting curves for DI (1), DE + DI (2), DE + DI + SI (3), DE only (2′) and SI only (3′). For details, see the text.

whole energy range. The cross sections measured at 114 mT (σ_{m2}) are corrected for the DI transmission (12) in order to obtain σ_{DI}.

Finally, both the DI and the SI contributions (curves 1 and 3, respectively) are subtracted from the spectra to obtain the DE apparent cross section, which is also fitted (curve 2′). The DE transmission factor (η_{DE}), which is determined by means of this curve, is seen to range from 40% just above the threshold down to 10% at high incident energies. σ_{DE} is determined as the difference between σ_{m1} and σ_{DI}, corrected for the DE transmission (12).

Typical working conditions are: ion current 20 nA, electron current 0.1–3 mA, electron beam sweeping speed 3.75 m s^{-1}, number of events per one sweep 0.1. The pressure is kept below 1×10^{-9} mbar in the collision chamber during the measurement, in order to reduce the background, which is due to interaction of primary ions with residual gas molecules. The energy of the ion beam (8 keV) is high enough to ensure the 100% efficiency of the channeltron detector.

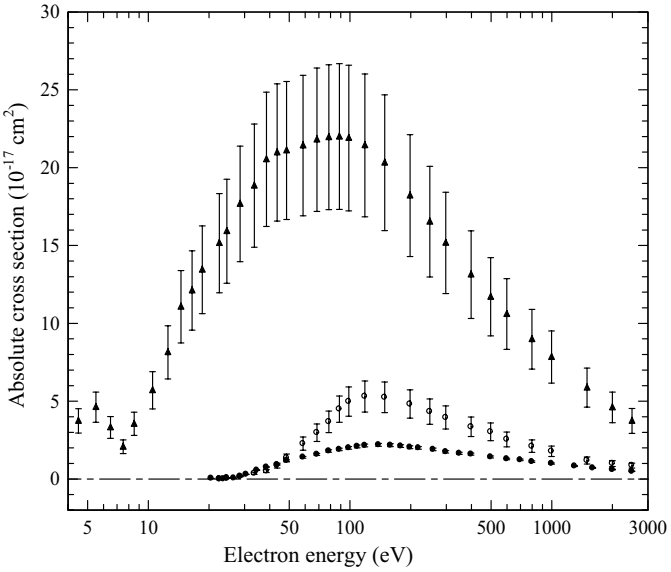

Figure 2. Absolute cross sections for electron impact simple ionization (σ_{SI}, •), dissociative ionization (σ_{DI}, ○), and dissociative excitation (σ_{DE}, ▲).

The total uncertainty (90% confidence limit) obtained as the quadratic sum of the systematic and statistical uncertainties, is found to be about 3.9% at the maximum of σ_{SI}. This includes all the uncertainties due to the determination of the experimental parameters (4). Additional uncertainties result from the procedures applied to estimate the transmission factor and to separate the DI and DE contributions. Finally, the total uncertainty around the cross section maximum is estimated to be 18.8% and 21% for σ_{DI} and for σ_{DE}, respectively.

3. Results and discussion

Absolute cross sections for processes (1–3) are shown in figure 2. They are also listed in table 1, together with the associated total uncertainties (90% confidence limit).

3.1. Simple ionization of O_2^+ (SI)

The maximum of σ_{SI} is found to be (2.20 ± 0.09) 10^{-17} cm^2 at the electron energy of 140 eV. The threshold energy for this process is estimated to be (24.0 ± 1.0) eV, or (36.2 ± 1.0) eV relative to the ground state of the neutral O_2 molecule. This value, which corresponds to the formation of the $O_2^{2+}\left(X^1\Sigma_g^+\right)$ is in a very good agreement with other available data: 35.88 eV as obtained by Hurley and Maslen (1961); (36.3 ± 0.5) eV obtained in an electron-ionization experiment by Dorman and Morrison (1963); (35.6 ± 0.3) eV in a crossed-beam experiment by Märk (1975), and (36.13 ± 0.02) eV in a threshold photoelectron coincidence experiment obtained by Hall *et al* (1992).

The total ionization cross section of O_2^+, which includes both simple ionization and dissociative ionization will be discussed later in this paper.

Table 1. Absolute cross sections (10^{-17} cm^2) for SI (σ_{SI}), DE (σ_{DE}) and DI (σ_{DI}) of O_2^+ by electron impact.

E_e(eV)	σ_{SI}	$\Delta\sigma_{SI}$	σ_{DE}	$\Delta\sigma_{DE}$	σ_{DI}	$\Delta\sigma_{DI}$
4.5	–	–	3.74	0.80	–	–
5.5	–	–	4.62	0.97	–	–
6.5	–	–	3.31	0.70	–	–
7.5	–	–	2.07	0.44	–	–
8.5	–	–	3.55	0.74	–	–
10.5	–	–	5.70	1.20	–	–
12.5	–	–	8.14	1.70	–	–
14.5	–	–	11.07	2.32	–	–
16.5	–	–	12.11	2.54	–	–
18.5	–	–	13.44	2.82	–	–
20.5	0.04	0.01	–	–	–	–
22.5	0.01	0.01	15.15	3.18	0.01	0.01
23.5	0.01	0.01	–	–	–	–
24.5	0.08	0.01	15.91	3.34	0.04	0.01
26.5	0.06	0.01	–	–	–	–
28.5	0.18	0.01	17.67	3.71	0.16	0.03
30.5	0.30	0.01	–	–	–	–
33.5	–	–	18.85	3.96	0.37	0.07
34.5	0.57	0.02	–	–	–	–
38.5	0.76	0.03	20.54	4.31	0.51	0.10
43.5	0.92	0.04	20.98	4.40	0.87	0.16
48.5	1.19	0.05	21.11	4.43	1.35	0.025
58.5	1.40	0.06	21.42	4.50	2.27	0.43
68.5	1.59	0.06	21.80	4.58	2.98	0.56
78.5	1.80	0.07	21.95	4.61	3.68	0.69
88.5	1.90	0.07	22.00	4.62	4.49	0.84
98.5	2.00	0.08	21.90	4.60	4.98	0.94
108.5	2.09	0.08	–	–	–	–
118.5	2.15	0.09	21.43	4.50	5.30	0.99
138.5	2.20	0.09	–	–	–	–
148.5	–	–	20.32	4.27	5.25	0.99
158.5	2.17	0.09	–	–	–	–
178.5	2.12	0.08	–	–	–	–
198.5	2.04	0.08	18.21	3.82	4.82	0.91
218.5	2.00	0.08	–	–	–	–
248.5	–	–	16.54	3.47	4.33	0.81
258.5	1.91	0.08	–	–	–	–
298.5	1.75	0.07	15.17	3.18	3.95	0.74
348.5	1.65	0.07			3.36	0.63
398.5	1.60	0.06	13.13	2.76	–	–
498.5	1.42	0.06	11.70	2.46	3.03	0.57
598.5	1.29	0.05	10.60	2.22	2.54	0.48
698.5	1.23	0.05	–	–	–	–
798.5	1.11	0.04	8.98	1.88	2.11	0.40
998.5	0.99	0.04	7.84	1.64	1.79	0.34
1298.5	0.84	0.03	–	–	–	–
1498.5	–	–	5.87	1.23	1.19	0.22
1598.5	0.71	0.03	–	–	–	–
1998.5	0.60	0.02	4.60	0.97	1.00	0.19
2498.5	0.50	0.02	3.73	0.78	0.87	0.16

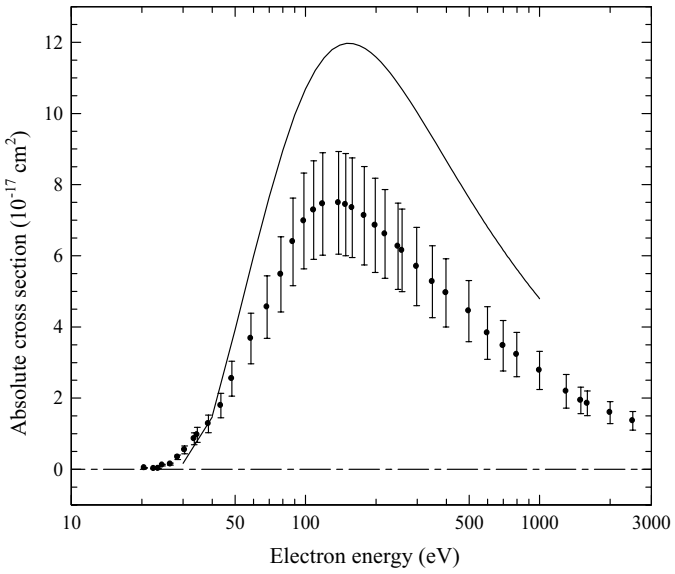

Figure 3. Absolute total ionization cross section ($\sigma_{SI} + \sigma_{DI}$): present experimental results (•) and prediction of Deutsch *et al* (2003) (—).

3.2. Dissociative ionization (DI)

The maximum of the cross section is found to be $(5.3 \pm 1.0)\ 10^{-17}$ cm^2 at the electron energy of 120 eV. The threshold energy is determined to be (25 ± 1) eV, that is, only 1 eV above the SI threshold energy. According to the potential curves calculated by Edvardsson *et al* (1998), this threshold should be of the order of 3 eV. This shift may indicate the presence of primary ions formed in the $a^4\Pi_u$ metastable state. Another threshold is clearly seen at 39 eV, or 51 eV relative to the ground state of the neutral O_2 molecule, which agrees well with the threshold $(50.0 \pm 0.5$eV) reported by Hagstrom and Tate (1941).

Absolute DI cross sections are more than a factor of 2 larger than the σ_{SI} in a wide energy range, indicating that doubly-charged O_2^{2+} ions dominantly dissociate before reaching the detector. This is justified by noting that the ion flight time from the collision region to the detector is about 12 μs, so that all the molecular states with the lifetime shorter than 12 μs should dissociate before reaching the detector. The comparison with the calculated lifetimes of O_2^{2+} levels (Fournier *et al* 1992, Lundqvist *et al* 1996, Edvardsson *et al* 1998), indicates that dications can survive only if they are formed in the metastable $X^1\Sigma_g^+$, $1^1\Sigma_u^-$ (v = 0, 1) and $1^1\Pi_g$ (v = 0–4) states. All the other O_2^{2+} states contribute to the DI signal, producing O^+ fragments in the ground or in the ^{2}D and ^{2}P excited levels.

The total ionization cross section, i.e. the sum of σ_{SI} and σ_{DI}, was estimated by means of the Deutsch–Märk semi-empirical model (Deutsch *et al* 2003). The two sets of data, experimental (present results) and calculated, are seen to agree well in shape (figure 3), but the calculated values overestimate experimental data by some 25% in the whole energy region.

The total ionization cross section is presented in the form of Bethe plot (figure 4). As for atoms and atomic ions, the product of the cross section and the electron energy exhibits the linear energy dependence in this presentation, which is seen to be valid above 50 eV.

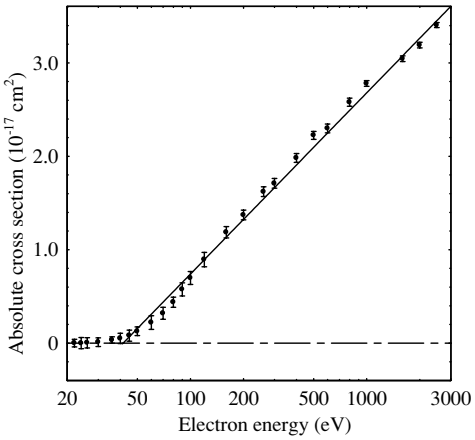

Figure 4. Bethe plot of the total ionization ($\sigma_{SI} + \sigma_{DI}$) cross section. The straight line is a fit of the data.

3.3. Dissociative excitation (DE)

The cross section maximum is found to be (22.0 ± 4.6) 10^{-17} cm^2 at the electron energy of 90 eV, that is, much larger than σ_{SI} and σ_{DI}. The threshold energy is determined to be (7.0 ± 1.0) eV. This value is in a good agreement with the value of (6.7 ± 0.2) obtained by Ehrhardt and Kresling (1967) and (6.8 ± 0.2) eV obtained by Peverall *et al* (2001).

However, below this energy, a small non-zero contribution can be seen. This can be explained either by the contribution of metastable vibrationally or electronically excited target ions, or by the process of resonant ion pair formation of O_2^+. An electron can be captured by O_2^+ to form O_2, which then dissociates to O^- and O^+, the positive ion being detected in our experiment. This process has been observed by Frost *et al* (1958) at electron energy as low as 5.2 eV.

Present DE data are compared (figure 5) with the data of Peverall *et al* (2001) obtained in an ion beam storage ring experiment. The data of Peverall *et al* are significantly higher in the whole energy region and in particular in the near threshold energy region. Similar disagreement in DE has been seen in our previous measurements on the CO^+ ion (Lecointre *et al* 2006) and no decisive argument could be invoked to explain this disagreement.

In the crossed beams experiment of Van Zyl and Dunn (1967) the cross section for total production of charged particles is measured while, in the present experiment, only one of the O^+ fragments (equation (3)) is detected, at a time. For the comparison of both sets of data, the present data are summed as follows: $\sigma_{SI} + \sigma_{DE} + 2\sigma_{DI}$. The agreement between the two sets of data (figure 6) is very good near the cross section maximum and in the whole high-energy region. At low energy, the data of Van Zyl and Dunn are somewhat higher, but the two sets of data agree within the associated total error bars.

3.4. Kinetic energy release (KER) distribution

Kinetic energy distributions are presented in figure 7, at electron energies of 4.5, 10.5, 13.5, 18.5, 38.5, 78.5, 148.5 and 498.5 eV, where magnetic scans were performed. With increasing incident electron energy, higher dissociative levels are reached, more energy is liberated in the

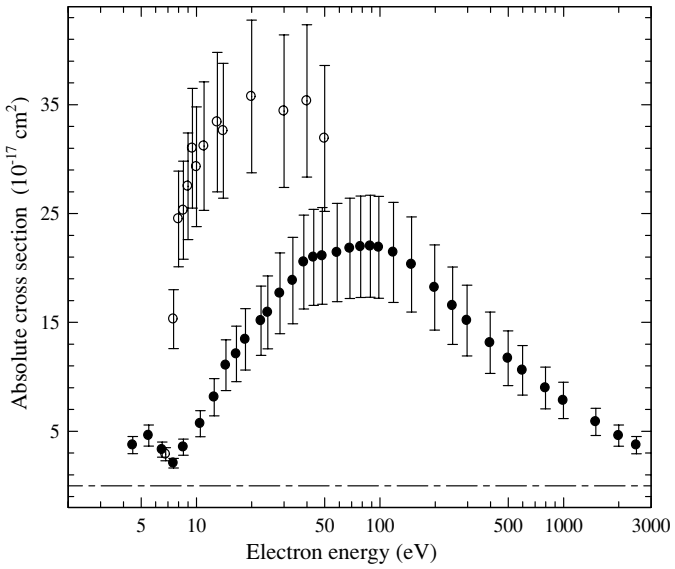

Figure 5. Absolute cross sections for electron impact dissociative excitation (σ_{DE}): present result (•) and Peverall *et al* (2001) (○).

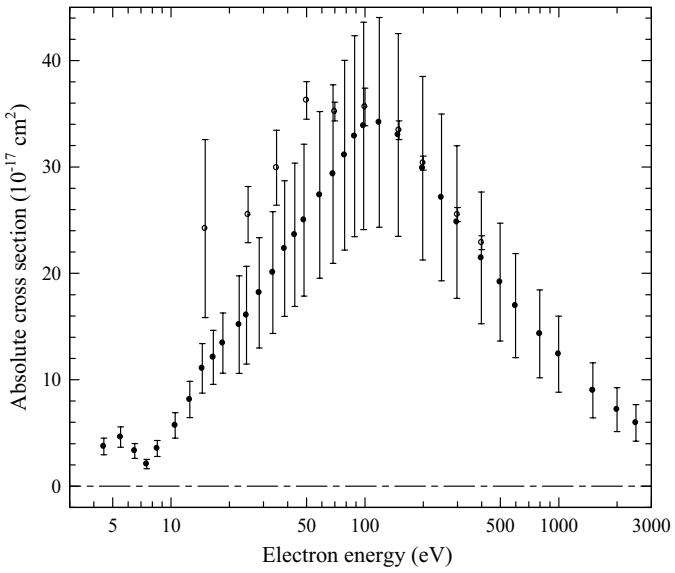

Figure 6. Cross section for total ion production ($\sigma_{SI} + \sigma_{DE} + 2\sigma_{DI}$): present result (•) and Van Zyl and Dunn (1967) (○).

centre-of-mass frame and the KERD becomes wider, extending progressively from 0 eV to almost 20 eV.

At the lowest incident electron energies (below the ionization threshold, figure 7(a)) a single peak is observed, which represents fragment energy distribution resulting from DE only.

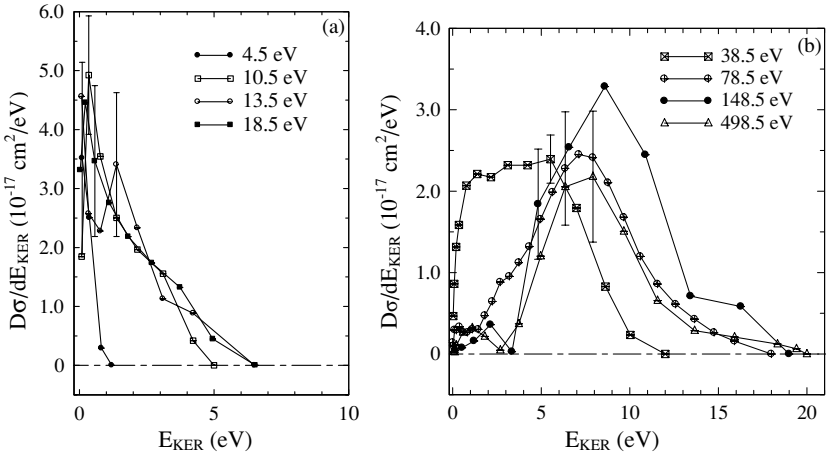

Figure 7. (a) Kinetic energy release distributions for selected electron energies, below the ionization threshold. (b) Kinetic energy release distributions for selected electron energies, above the ionization threshold.

At higher electron energies (figure 7(b)), a weak contribution appears at 38.5 eV, which cannot be isolated, the KERD expands further to higher energies due to the additional DI contribution.

At low electron energies, the presence of fragments with near zero kinetic energy indicates that they originate from O_2^+ predissociative states (Locht *et al* 1974). It was also shown (Momigny 1980) that the bonding $b^4\Sigma_g^-$ level (v = 4, 5, 6) predissociates via the repulsive $^4\Pi_g$ and $^4\Sigma_g^+$ states with very low excess energy. Excess energy of about 1 eV is associated to the predissociation of the $B^2\Sigma_g^-$ level (Zhukov *et al* 1990). In addition, some O_2 Rydberg levels ($^3\Pi_u$, $^2\Delta_g$) can also give low kinetic energy fragments by dissociative autoionization (Bakker and Parker 2000).

KERDs have been tentatively decomposed into their partial contributions by fitting the data with Gaussian functions for DI. For DE, we adopted the function fitting the KERD at 13.5 eV. Both the individual contributions and their sum are shown (figure 8) for 78.5 eV electron energy. In this case, five contributions are isolated, centred around 0.5, 1.5, 2.5, 7.3 and 13 eV. The four lowest ones can be associated to DE, the fifth to DI. As a check, the ratio of the DE and DI contributions confirmed the result of the processes separation procedure described above.

It is worth mentioning that published results usually refer to the kinetic energy of a single fragment, so that they must be multiplied by 2 for comparison with present estimations, which correspond to the total kinetic energy released to both fragments (10). This correction has been applied in table 2, which summarizes both the experimental and calculated data.

Eland and Duerr (1998) analysed dissociation resulting from electron impact ionization of O_2. Below 40 eV electron energy, 14 KER peaks were identified, 5 with low energy (via the $b^4\Sigma_g^-$, $B^2\Sigma_g^-$, $3^2\Pi_u$, $c^4\Sigma_u^-$ and $^2\Sigma_u^-$ states) and 9 with larger fragment kinetic energies extending from 5.1 to 13 eV, some of them probably from DI. Cho and Lee (1996) applied the time-of-flight coincidence technique to measure the O^+ kinetic energy distribution from electron impact double ionization of O_2. A similar distribution extending from 2 to 11 eV, showed local maxima at about 4, 6 and 9 eV. The agreement between them is satisfactory, bearing in mind the different experimental methods involved.

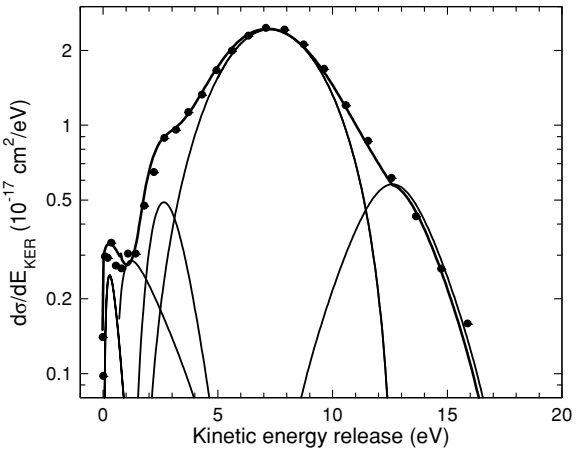

Figure 8. Contribution of DE and DI to the O^+ KERD at 78.5 eV electron energy.

Table 2. Total fragment kinetic energy peak locations (eV).

	Present results	Eland and Duerr (1998)	Zhukov *et al* (1990)	Cho and Lee (1993)	Stockdale and Deleanu (1973)
DE	0.5	Low	Low		
	1.5				1.4
	2.5		2		
	5	5.1	4		4
		5.9	6		6
		6.7			
	7.3	7.6			
		8.3		8	
		10.7	10		10
		11.5			
DI	13	12.6		12	
		13.0			
	15.5		15	18	

4. Summary

Electron impact ionization and dissociation of the O_2^+ molecular ion was studied in a crossed beams experiment. Partial absolute cross sections were determined for simple ionization (SI), dissociative ionization (DI) and dissociative excitation (DE) in the electron energy range from threshold to 2.5 keV, for the first time. The total KERD of product fragments, estimated for several electron energies, were seen to extend up to about 20 eV. Various contributions to the KERD were identified and they were found to be in satisfactory agreement with published data.

Acknowledgments

The authors acknowledge the financial support of the Association Euratom-Belgian State and the technical support of C Alaime and D Dedouaire. They are indebted to A Lepadellec, N Vaeck and R Locht for valuable discussions.

References

Bahati E M, Jureta J J, Belic D S, Cherkani-Hassani H, Abdellahi M O and Defrance P 2001 *J. Phys. B: At. Mol. Opt. Phys.* **34** 2963

Bakker L G and Parker D H 2000 *J. Chem. Phys.* **112** 4037

Cho H and Lee J H 1996 *Phys. Rev.* A **54** 3665

Defrance P, Brouillard F, Claeys W and Van Wassenhove G 1981 *J. Phys. B: At. Mol. Phys.* **14** 103

Deutsch H, Becker K, Defrance P, Onthong U, Probst M, Matt S, Scheier P and Märk T D 2003 *Int. J. Mass Spectrom.* **223–224** 639

Dorman F H and Morrison J D 1963 *J. Chem. Phys.* **39** 1906

Edvardsson D, Lunell S, Rakowitz F, Marian C M and Karlsson L 1998 *Chem. Phys.* **299** 203

Ehrhardt H and Kresling A 1967 *Z. Naturforsch.* **22a** 2036

Eland J H D and Duerr E J 1998 *Chem. Phys.* **229** 1

Fournier J, Fournier P G, Langford M L, Mousselman M, Robbe J M and Gandara G 1992 *J. Chem. Phys.* **96** 3594

Hagstrom H D and Tate J T 1941 *Phys. Rev.* **59** 354

Hall R I, Dawber G, McConkey A, MacDonald M A and King G C 1992 *Phys. Rev. Lett.* **68** 2751

Hurley A C and Maslen V W 1961 *J. Chem. Phys.* **34** 1919

Lecointre J, Belic D S, Cherkani-Hassani H, Jureta J J and Defrance P 2006 *J. Phys. B: At. Mol. Opt. Phys.* **39** 3275

Locht R and Schopman J 1974 *Int. J. Mass Spectrom. Ion Processes* **15** 361

Lundqvist M, Edvardsson D, Baltzer P, Larson M and Wannberg B 1996 *J. Phys. B: At. Mol. Opt. Phys.* **29** 499

Märk T D 1975 *J. Chem. Phys.* **42** 3731

Momigny J 1980 *J. Chim. Phys.* **77** 725

Peverall R *et al* 2001 *J. Chem. Phys.* **114** 6679

Stockdale J A D and Deleanu L 1973 *Chem. Phys. Lett.* **26** 596–600

Van Zyl B and Dunn G H 1967 *Phys. Rev.* **163** 43

Zhukov A I, Zavilopulo A N, Snegursky A V and Shpenik O B 1990 *J. Phys. B: At. Mol. Opt. Phys.* **23** 2373S